Theory of the nodal nematic quantum phase transition in superconductors

Eun-Ah Kim,[1] Michael J. Lawler,[2] Paul Oreto,[1] Subir Sachdev,[3] Eduardo Fradkin,[3] and Steven A. Kivelson[1]
[1]*Department of Physics, Stanford University, Stanford, California 94305, USA*
[2]*Department of Physics, University of Toronto, Toronto, Ontario, Canada*
[3]*Department of Physics, University of Illinois at Urbana-Champaign, 1110 West Green Street, Urbana, Illinois 61801-3080, USA*
(Received 15 February 2008; published 22 May 2008)

We study the character of an Ising nematic quantum phase transition deep inside a d-wave superconducting state with nodal quasiparticles in a two-dimensional tetragonal crystal. We find that, within a $1/N$ expansion, the transition is continuous. To leading order in $1/N$, quantum fluctuations enhance the dispersion anisotropy of the nodal excitations and cause strong scattering, which critically broadens the quasiparticle (qp) peaks in the spectral function, except in a narrow wedge in momentum space near the Fermi surface where the qps remain sharp. We also consider the possible existence of a nematic glass phase in the presence of weak disorder. Some possible implications for cuprate physics are also discussed.

DOI: 10.1103/PhysRevB.77.184514 PACS number(s): 74.72.−h, 73.43.Nq, 74.20.De, 74.25.Dw

I. INTRODUCTION

In this paper, we study the nematic to isotropic quantum phase transition (QPT) deep within the d-wave superconducting phase of a quasi-two-dimensional tetragonal crystal. "Nematic" refers to a broken symmetry phase in which the fourfold rotational symmetry of the crystal is broken down to a twofold symmetry. More specifically, it is an "Ising nematic," which spontaneously breaks the discrete rotational symmetry of the tetragonal crystal to an orthorhombic subgroup, $C_{4v} \to C_{2v}$, while retaining translational symmetry. The superconducting order opens a gap in the quasiparticle excitation spectrum, except at four gapless nodal points, but these nodal quasiparticles (qps) strongly couple to the nematic order parameter fluctuations. In the nematic phase, these nodes are displaced from the relevant symmetry directions by an amount proportional to the nematic order parameter, as shown in Fig. 1. We derive a phenomenological theory to describe this "nodal nematic QPT" consisting of a nematic mode coupled to the nodal qps of the d-wave superconductor.

Our motivation to investigate this problem is twofold: First, there is now considerable experimental evidence that a nodal nematic phase occurs in at least some "underdoped" cuprate superconductors, so this study has potential relevance to the transition from this state to the isotropic state in these materials. The best evidence of this comes from measurements[1] of strongly temperature dependent transport anisotropies in underdoped $YBa_2Cu_3O_{6+\delta}$ and more recent (and more direct) neutron scattering experiments in underdoped $YBa_2Cu_3O_{6.45}$ (YBCO).[2] Specifically, the spontaneous onset of one-dimensional incommensurate spin modulations in the neutron experiments is clear evidence of an isotropic-to-nematic transition with transition temperature $T_N \sim 150$ K. For $\delta=0.45$, T_N is greater than the superconducting $T_c=35$ K. However, at a higher O concentration, $\delta \gtrsim 0.7$, both neutron scattering and transport experiments see no evidence of a transition to a nematic phase down to the lowest temperatures.[1,3–6] It is thus reasonable to assume that $T_N(\delta) \to 0$ for a critical value, $0.45 < \delta_c < 0.7$, with a QPT at $\delta = \delta_c$ inside the SC phase.[5–11] The extent to which nematic phases are generic to the cuprates is a question that is beyond the scope of the present study. However, Matsuda *et al.*[12] recently reported that the "fluctuating stripe" phase of underdoped (diagonal) $La_{2-x}Sr_xCuO_4$ (with $x=0.04$) is actually a nematic phase. Moreover, scanning tunneling microscopy (STM) studies by Howald *et al.*[13] and Kohsaka *et al.*[14] have revealed a glassy phase with nematic domains in underdoped $Bi_2Sr_2CaCu_2O_{8+\delta}$.

Second, the topic of quantum critical points (QCPs) in two-dimensional (2D) systems with itinerant fermions has been and continues to be a topic of broad interest. Here, we study a new QCP in a 2D itinerant fermion system. In general, the presence of gapless fermions at the Fermi surface makes the study of this topic theoretically challenging. Since gapless fermions interact with massless bosons associated with order parameter fluctuations, this interaction affects both low energy degrees of freedom, making it difficult to obtain a correct description of the critical physics. Simplifications occur when one considers nodal fermions that are gapless only at four nodal points of the underlying Fermi surface in a d-wave superconductor. The limited phase space for the gapless fermions restricts the possibilities for scattering mechanisms, permitting a controlled analysis.

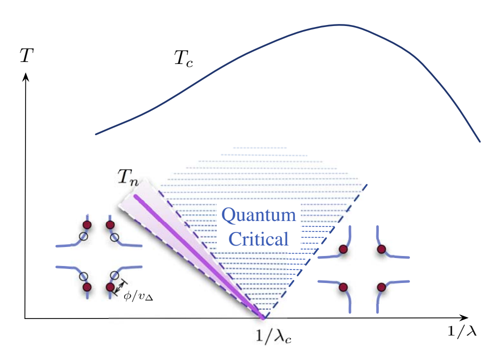

FIG. 1. (Color online) Quantum critical point at $\lambda=\lambda_c$, separating the nodal nematic phase for $\lambda^{-1}<\lambda_c^{-1}$ from the symmetric phase, and its quantum critical fan. T_c and T_n are the superconducting and nematic critical temperatures and the (purple) wedge corresponds to the thermal critical regime.

Electronic nematic phases were first predicted to occur in doped Mott insulators[5] and have now been experimentally observed in a number of different systems. In addition to YBCO, they have been discovered in transport experiments in semiconductor heterostructures[15] and in the bulk transition metal oxide $Sr_3Ru_2O_7$.[16] While in all cases the thermal transition to the nematic phase appears to be continuous, the character of the quantum transition at zero temperature is less clear and, at least in the case of $Sr_3Ru_2O_7$,[16] appears to be first order. However, interesting universal physics can be expected in the case of a continuous transition.

Vojta *et al.*[9,10] analyzed various types of ordering transitions in a nodal superconductor, including Ising nematic ordering. They employed an ϵ expansion ($\epsilon=3-d$) to derive perturbative renormalization group (RG) flows near the decoupled fixed point, $\lambda=0$. In the nematic case, they found runaway flows, which they tentatively interpreted as a fluctuation induced first order transition. Of course, a runaway flow can also imply breakdown of perturbation theory.

In this paper, we directly work in $d=2$ and use a large N theory to access a nontrivial critical point at finite coupling λ_c. This is achieved by generalizing the problem to one in which there are N "flavors" of nodal qps (with the physical $N=2$ case corresponding to two spin polarizations).[17] In the large N limit, we present a theory of the nodal nematic QPT,[18] whose critical behavior should be smoothly and systematically corrected by the $1/N$ expansion.[19–22] We find the following: (a) the quantum phase transition is continuous, with nontrivial critical exponents that we compute for $N\to\infty$, (b) the transition occurs at a *finite* critical coupling between the nodal qps and the nematic order parameter, so it is inaccessible by perturbation theory; (c) the anisotropy of the nodal qp dispersion strongly influences the interplay between the critical fluctuations and the qps. We also speculate on the implications of this theory to the phenomenology of nodal qps in cuprates. With minor changes, this theory also applies to a possible electronic hexatic QPT in graphene and similar systems.[24]

The paper is organized as follows. In Sec. II, we introduce the model and discuss its symmetries. The effective theory of the nematic order parameter is derived in the large N limit in Sec. III. In Sec. IV, we discuss the behavior of the nodal quasiparticles at and near the nematic quantum critical point. In Sec. V, we give a qualitative presentation of the physics of a nematic glass and how it affects the spectrum of a nodal quasiparticle, leading to a Fermi arc phenomenology in the quasiparticle spectral function. In Sec. VI, we discuss a number of important open problems.

II. MODEL

The effective Lagrangian that describes the coupling of the nodal fermionic qps to the nematic order parameter is $\mathcal{L}=\mathcal{L}_\Psi+\mathcal{L}_{\rm int}+\mathcal{L}_\phi$, where $\mathcal{L}_\Psi$ is the linearized nodal qp Lagrangian in a pure $d_{x^2-y^2}$ SC:

$$\mathcal{L}_\Psi=\sum_{n,\alpha}\bar{\Psi}_{n,\alpha}\left(\partial_\tau-i\tau_3\vec{v}_F^n\cdot\vec{\nabla}-i\tau_1\vec{v}_\Delta^n\cdot\vec{\nabla}\right)\Psi_{n,\alpha}. \tag{2.1}$$

Here,

$$\Psi_{n,\alpha}(\vec{p})\equiv\begin{pmatrix}c_{\vec{K}_n+\vec{p},\alpha}\\ \epsilon_{\alpha\beta}c^\dagger_{-(\vec{K}_n+\vec{p}),\beta}\end{pmatrix} \tag{2.2}$$

are two-component Nambu spinors representing the nodal qps for node index $n=1,2$ and $\alpha,\beta=1,\ldots,N$ are $Sp(N/2)$ flavor indices which, for $N=2$, correspond to the qp spin polarizations since $Sp(1)\simeq SU(2)$. Equation (2.2) represents nodal qps at momentum positions $\vec{p}$ relative to each pair of nodes at $\vec{K}_1=(K,K)$ and $\vec{K}_2=(-K,K)$ for $n=1,2$, respectively, and

$$\vec{v}_F^n=\vec{\nabla}_k\epsilon_k|_{\vec{k}=\vec{K}_n},\qquad \vec{v}_\Delta^n=\vec{\nabla}_k\Delta_k|_{\vec{k}=\vec{K}_n} \tag{2.3}$$

are velocities normal and tangential to the Fermi surface (FS). Note that we investigate our model for general values of v_F and v_Δ. We use τ_1 and τ_3 to denote 2×2 Pauli matrices acting on the Nambu spinors. The Lagrangian for the nematic order parameter ϕ is

$$\mathcal{L}_\phi=\frac{m^2}{2}\phi^2+\frac{1}{2}[(\partial_\tau\phi)^2+c^2(\nabla\phi)^2]+\frac{u}{4N}\phi^4+\cdots, \tag{2.4}$$

where the ellipsis represents higher order terms in powers of the nematic order parameter field ϕ. We assume that $u>0$ and that $m^2>0$, i.e., in the absence of coupling to the nodal qps, the system is in its isotropic phase, $\langle\phi\rangle=0$, and the nematic mode is gapped. The interaction term that couples the nematic order parameter to a fermion bilinear is

$$\mathcal{L}_{\rm int}=\frac{\lambda}{\sqrt{2N}}\sum_{n,\alpha}\phi\bar{\Psi}_{n,\alpha}\tau_1\Psi_{n,\alpha}, \tag{2.5}$$

which has a well defined large N limit.[19–22] This model has the discrete symmetry $(\phi\to-\phi,\vec{p}\to-\vec{p},\Psi\to\tau_2\Psi)$. The combination of this discrete symmetry with the implicit symmetry of the Nambu notation and the twofold rotation symmetry associated with $(\Psi_1\leftrightarrow\Psi_2,k_x\leftrightarrow k_y)$ amounts to C_{4v} symmetry. Should $\langle\phi\rangle\neq0$, the position of the nodes shift in the $\vec{v}_\Delta^n$ direction and the C_{4v} symmetry is spontaneously broken down to C_{2v} associated with $(\Psi_1\leftrightarrow\Psi_2,k_x\leftrightarrow k_y)$ (see Fig. 1).

The interaction in Eq. (2.5) has the form of a Dirac fermion current coupled to one component of a vector gauge field. Couplings of this type have been studied in the context of gauge theoretic approaches to nodal fermions and phase fluctuations.[25–27] However, in the case at hand, the microscopic theory *does not have a local gauge invariance* associated with the nematic field ϕ but, instead, only has a global *discrete* symmetry which can be spontaneously broken.

Since the coupling makes the tangential and normal directions to the FS inequivalent, one *must* consider an anisotropic dispersion, $v_F/v_\Delta\neq1$. Indeed, in previous studies of quantum criticality with Dirac-like fermions, an effective rotational symmetry about the nodal point, $v_F/v_\Delta\to1$, was shown to be an emergent property of the fixed point in the sense that anisotropy is perturbatively irrelevant; this is not true in the present problem, and indeed, we find a number of qualitatively new features of the critical theory which derive from this anisotropy.

The fact that v_F and v_Δ have different physical origins implies that there is no reason *a priori* to expect the existence of even an approximate symmetry $v_F = v_\Delta$. Indeed, experimentally, it is well known that the degree of anisotropy is extreme: $v_F/v_\Delta \sim 19$ for BSCCO from thermal conductivity[29] and ARPES (Ref. 30) and $v_F/v_\Delta \sim 14$ for YBCO from thermal conductivity.[29] After we formulate our theory for general values of v_F and v_Δ, we investigate the specific case that corresponds to linearizing the phenomenological band structure of Norman *et al.*[30]

III. ORDER PARAMETER THEORY

We will now proceed to study the behavior in the large N limit of the theory of nodal fermions coupled to a nematic order parameter theory presented in the previous section. As it is standard in the large N limit, we proceed to formally integrating out the fermions and obtain the resulting effective action for the nematic order parameter field.[19,21,22] In the large-N limit, the resulting bosonic path integral:

$$\mathcal{Z} = \int \mathcal{D}\phi e^{-S_{\text{eff}}[\phi]}, \tag{3.1}$$

will be dominated by the saddle point solution to the effective action $S_{\text{eff}}[\phi]$ and is amenable to a controlled $1/N$ expansion to evaluate the effects of fluctuations. In imaginary time, the full effective action $S_{\text{eff}}[\phi]$ has the standard form

$$S_{\text{eff}}[\phi] = \int d^3x \left[\frac{m^2}{2}\phi^2 + \frac{1}{2}[(\partial_\tau \phi)^2 + c^2(\nabla\phi)^2] + \frac{u}{4N}\phi^4 \right] - N\sum_n \ln \text{Det}\left(\partial_\tau - i\tau_3 \vec{v}_F^n \cdot \vec{\nabla} - i\tau_1 \vec{v}_\Delta^n \cdot \vec{\nabla} + \frac{\lambda}{\sqrt{2N}}\tau_1\phi \right). \tag{3.2}$$

The fermion determinant in Eq. (3.2) represents the sum of fermion bubble Feynman diagrams. Since the action of the nodal fermions has the structure of an anisotropic Dirac theory with a coupling to the nematic order parameter ϕ, each bubble diagram involves a trace over a product of Dirac fermion propagators with the appropriate insertions of the matrices τ_1 dictated by the form of the coupling. This is a standard procedure which obviates the need to present the well known intermediate steps. We will thus only present the main results of these calculations.

Upon rescaling the order parameter $\phi \to \sqrt{N}\phi$, it is apparent that the effective action for the rescaled field ϕ has the form $NS_{\text{eff}}[\phi]$. Hence, in the large-N limit, the path integral is dominated by the solution to the saddle point equations for the effective action $S_{\text{eff}}[\phi]$ and its fluctuations. When expanded in powers of ϕ, the contribution of the fermion determinant introduces a negative contribution to the quadratic term that is proportional to λ^2 in the effective action $S_{\text{eff}}[\phi]$.[19–21] This allows for the spontaneous symmetry breaking driven by the coupling constant λ. In theories of this type,[19,21,22] there is a critical coupling strength λ_c, beyond which ϕ gains a finite expectation value due to the spontaneous symmetry breaking. The critical value of the coupling constant, which is the location of the quantum phase transition, depends on the bare mass of the nematic mode and the UV cutoff. If we use a sharp UV cutoff Λ, in the large-N limit, we obtain

$$\lambda_c^2 = [2\pi^2/\ln 2](m^2 v_F v_\Delta/\Lambda). \tag{3.3}$$

For $\lambda^2 < \lambda_c^2$, the symmetry is unbroken and $\langle\phi\rangle = 0$. However, for $\lambda^2 > \lambda_c^2$, a nonzero expectation value $\langle\phi\rangle$ is obtained by minimizing $S_{\text{eff}}[\phi]$. This can be achieved by solving the saddle point equation:

$$m^2\langle\phi\rangle = -\frac{\lambda}{\sqrt{2N}}\sum_{n,\alpha}\langle\bar{\Psi}_{n,\alpha}\tau_1\Psi_{n,\alpha}\rangle. \tag{3.4}$$

For λ close to λ_c, the solution of Eq. (3.4) satisfies

$$\langle\phi\rangle \propto (\lambda - \lambda_c)^{1/2}. \tag{3.5}$$

Thus, in the large-N limit, we find a continuous quantum phase transition, i.e., a quantum critical point, separating the weak coupling isotropic phase at $\lambda < \lambda_c$ from a strong coupling phase at $\lambda > \lambda_c$. The critical exponent of the order parameter of Eq. (3.5), which is $1/2$, obtained in the large-N limit will be corrected order by order in the $1/N$ expansion.[19,21] Within the $1/N$ expansion, the corrections to the value of this and other critical exponents of this theory follow from the resummation (exponentiation) of the infrared divergent $1/N$ perturbation theory. This procedure can also be viewed as a construction of a fixed-point theory (and its associated renormalization group) order by order in the $1/N$ expansion, which is a standard procedure in relativistically invariant theories of Dirac fermions.[19,21]

In the present problem, Lorenz invariance is explicitly absent due to both the velocity anisotropy, which is parametrized by the velocity ratio v_F/v_Δ, and the form of the coupling between the nematic order parameter ϕ and the Dirac fermions. Lack of this invariance changes the physics in dramatic ways. As noted above, Vojta *et al.* studied the quantum critical behavior of a similar system by means of a perturbative RG analysis at fixed N near the critical (renormalizable) dimension $D=3+1$ by using an ϵ expansion.[9,10] Due to the combined effects of the velocity anisotropy and the anisotropic coupling, they found that the perturbative RG has runaway flows, signaling the breakdown of perturbation theory. Following a standard analysis (see, for instance, Refs. 21 and 23, these authors interpreted this runaway flow as an indication of a fluctuation induced first order transition. Instead, in the large-N theory that we present here, we find that, at fixed dimension $D=2+1$ but for very large N, the quantum phase transition is continuous and has a finite renormalized velocity anisotropy which plays a key role.[28] This behavior also contrasts with that of more nearly Lorenz invariant models, such as the QED$_3$-type models studied in Refs. 25–27, where a small velocity anisotropy was found to be either irrelevant or redundant.

We will now proceed with the analysis of this theory in the large-N limit. The leading quantum fluctuations at large N are obtained by expanding the effective action to quadratic order about the saddle point (see, for instance, Ref. 31). This standard procedure, when applied to the present problem which breaks Lorentz invariance, introduces two separate energy scales associated with any given momentum $\vec{p}$

$$E_1(\vec{p}) = \sqrt{v_F^2 p_x^2 + v_\Delta^2 p_y^2} \text{ and } E_2(\vec{p}) = \sqrt{v_F^2 p_y^2 + v_\Delta^2 p_x^2}, \tag{3.6}$$

where $E_1(p_x,p_y)=E_2(p_y,p_x)$. In terms of $E_1(\vec{p})$ and $E_2(\vec{p})$, the Gaussian action $S^{(2)}[\varphi]$ for the fluctuations of the nematic mode $\varphi(x)$ defined by $\varphi(x)\equiv\frac{m}{\lambda_c}[\phi(x)-\langle\phi\rangle]$, which takes the following form on the disordered side ($\lambda<\lambda_c$) of the critical point:

$$S^{(2)}[\varphi] = \int \frac{d^2p d\omega}{(2\pi)^3}\frac{1}{2}\{(\lambda_c^2-\lambda^2) + \kappa(\omega^2 + c^2\vec{p}^2) + \gamma[\sqrt{\omega^2 + v_F^2 p_x^2 + v_\Delta^2 p_y^2} + (v_\Delta \leftrightarrow v_F)]\}|\varphi(p)|^2, \tag{3.7}$$

where $\kappa\equiv\lambda_c/m^2$ and $\gamma\equiv\lambda_c^2/64v_F v_\Delta$. The quartic and higher order terms in fluctuations have coefficients which are[21,22] down by powers in $1/N$. Here, we will only treat the physics to leading order in this expansion.[32]

We can analyze the effective action in Eq. (3.6) from the viewpoint of scaling theory. Clearly, at criticality ($\lambda=\lambda_c$), the bare dynamical terms in Eq. (2.4) are irrelevant, because they have a larger dimension than the nonlocal term generated by integrating out the nodal fermions. The scaling dimension of the nematic field φ, as traditionally defined, is $\dim[\varphi]=(d+z-2+\eta)/2$, with the space dimension d, the dynamic critical exponent z, and the anomalous dimension η. In the present case, $\dim[\varphi]=1$ and $z=1$ is inherited from the Dirac-like spectrum of the fermions. This can then be interpreted as a large anomalous dimension $\eta=1$.[34] As a result of this scaling, all *local* interaction terms of higher order in φ are (sometimes dangerously) *irrelevant* operators. (This is in contrast to a local φ^4 theory in which the $u\varphi^4$ term is relevant for $d<3$ at the Gaussian fixed point, so long as $z<2$, making the fixed point unstable.) Nonlocal interactions are also generated by integrating out the fermions, which, presumably, lead to $O(1/N)$ corrections to the various critical exponents. Away from criticality, the correlation length scales as $\xi\sim|\lambda_c-\lambda|^{-\nu}$, with $\nu=1$. To the extent that scaling holds, $T_c\sim(\lambda-\lambda_c)$ for $\lambda>\lambda_c$ ($\nu z=1$). The resulting phase diagram, with a v-shaped quantum critical fan, is sketched in Fig. 1.

We compute the spectral response of the nematic mode by an analytic continuation of the effective action Eq. (3.6) to real time. The irrelevant terms in the effective action can be set to zero for energies small compared to γ/κ. In Fig. 2, we show the spectral function of the nematic mode φ at criticality:

$$B(\vec{p},\omega) \equiv -2\,\mathrm{sgn}(\omega)\mathrm{Im}\,G(\vec{p},\omega), \tag{3.8}$$

for the φ propagator

$$G(\vec{p},\omega) = \left[\gamma\sqrt{-\omega^2 + E_1(\vec{p})^2} + \gamma\sqrt{-\omega^2 + E_2(\vec{p})^2}\right]^{-1}, \tag{3.9}$$

where we defined projectors

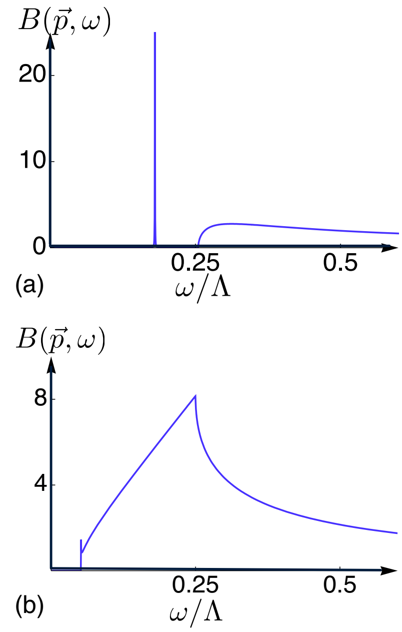

FIG. 2. (Color online) The nematic mode spectral function $\tilde{B}(\omega,\vec{p})$ plotted as a function of energy ω/Λ at momentum $\vec{p}=(0.05\Lambda/v_F,0.15\Lambda/v_F)$, where Λ is a UV cutoff and v_F is the Fermi velocity. (a) Isotropic case $v_F=v_\Delta=v$. (b) Anisotropic case $v_F/v_\Delta=19.5$. Notice how the singular feature at $\omega=v\sqrt{(p_x^2+p_y^2)}=0.16\Lambda$ for an isotropic dispersion splits into two features at $\omega=E_1(\vec{p})\sim0.05$ and $\omega=E_2(\vec{p})\sim0.15$ for an anisotropic dispersion. See Eq. (3.9).

$$\mathcal{P}_1 = 1 - \frac{v_\Delta^2 p_y^2}{-\omega^2 + E_1(\vec{p})^2},\quad \mathcal{P}_2 = 1 - \frac{v_\Delta^2 p_x^2}{-\omega^2 + E_2(\vec{p})^2}. \tag{3.10}$$

The spectral function of Eq. (3.8) contains contributions from a pole and from branch cuts. When the dispersion is isotropic, the nematic mode pole is at $\omega=v|\vec{p}|/\sqrt{2}$ with residue $Z=1/4$ and there is a threshold at $\omega=v|\vec{p}|$ for the continuum due to the branch cut. [See Fig. 2(a)[30]]. However, the dispersion anisotropy Notice that the dispersion anisotropy $\alpha>0$ ($v_F>v_\Delta$) completely alters the analytic structure of the nematic mode spectral function. First of all, the pole approaches the continuum with a reduced residue.[30] Moreover, the threshold energy scale for the continuum at $\omega=v|\vec{p}|$ associated with given momentum $\vec{p}|$ for an isotropic dispersion, splits into features at two energy scales $E_1(\vec{p})$ and $E_2(\vec{p})$ [See Fig. 2(b)]. The spectral function $B(\vec{q},\omega)$ can, in principle, be measured with momentum resolved inelastic x-ray scattering. Observation of a nematic mode spectral function with two distinct energy scales associated with a given momentum will serve as direct evidence for nodal nematic criticality. Moreover, the nontrivial analytic structure of the nematic mode spectral function results in momentum dependent scattering for quasiparticles.

IV. PROPERTIES OF NODAL FERMIONS AT CRITICALITY

The critical nematic fluctuations have drastic effects on the nature of nodal fermions. To illustrate this, here we will discuss the single particle spectral function at the nodal nematic QCP, which is defined in the vicinity of each node $n=1,2$ as

$$A_n(\vec{p},\omega) \equiv -2\,\mathrm{sgn}(\omega)\mathrm{Im}[\mathcal{G}_{n,11}(\vec{p},\omega)]. \tag{4.1}$$

Here, $\mathcal{G}_{n,11}(\vec{p},\omega)$ is the (11) component of the (2×2) Nambu matrix time ordered qp propagator:

$$\hat{\mathcal{G}}_n(\vec{p},\omega) \equiv -i\langle \Psi_n(\vec{p},\omega)\bar{\Psi}_n(\vec{p},\omega)\rangle. \tag{4.2}$$

Note in the rest of this section that we will focus on the vicinity of the $n=1$ node and omit the subscript $n=1$ to simplify the notation.

A matrix-valued qp self-energy $\hat{\Sigma}(\vec{p},\omega)$ best characterizes the effect of critical nematic fluctuations on the single fermion spectral function. We can then express $A(\vec{p},\omega)$ in terms of $\hat{\Sigma}$ in the standard manner. In the presence of $\hat{\Sigma}$, the Nambu matrix propagator for the nodal Fermions $\hat{\mathcal{G}}$ is given by $\hat{\mathcal{G}}^{-1}=\hat{\mathcal{G}}_0^{-1}-\hat{\Sigma}$, where $\hat{\mathcal{G}}_0(\vec{p},\omega)=(\omega\mathbb{I}-v_F p_x\tau_3-v_\Delta p_y\tau_1)^{-1}$ is the Nambu matrix propagator of the free nodal fermion theory. By decomposing the matrix valued self-energy in a basis of Pauli matrices as $\hat{\Sigma}(\vec{p},\omega)\equiv\Sigma^{(0)}\mathbb{I}-\Sigma^{(1)}\tau_3+\Sigma^{(2)}\tau_1$, the associated single particle spectral function is

$$A(\vec{p},\omega) = -2\,\mathrm{sgn}(\omega) \times \mathrm{Im}\left[\frac{(\omega-\Sigma^{(0)})+(v_F p_x-\Sigma^{(1)})}{(\omega-\Sigma^{(0)})^2-(v_F p_x-\Sigma^{(1)})^2-(v_\Delta p_y+\Sigma^{(2)})^2}\right]. \tag{4.3}$$

From Eq. (4.3), one can understand the effect of the different components of $\hat{\Sigma}$ on the physical properties of the fermions.

To order $1/N$, the (2×2) qp self-energy matrix at the QCP is

$$\hat{\Sigma}(\vec{p},\omega) = \frac{i\lambda_c^2}{2N}\int \frac{d^2k}{(2\pi)^2}\frac{d\omega'}{2\pi}\tau_1\hat{\mathcal{G}}_0(\vec{k},\omega')\tau_1 G(\vec{p}+\vec{k},\omega+\omega'), \tag{4.4}$$

where $G(\vec{k},\omega)$ is the large-N nematic mode propagator of Eq. (3.8). It can easily be checked that the components $\Sigma^{(i)}(\vec{p},\omega)$ in the Pauli matrix basis are proportional to $\omega, v_F p_x, v_\Delta p_y$, respectively, for $i=0,1,2$. As a result, the spectral function Eq. (4.3) scales with ω and $\vec{p}$ (up to logarithmic corrections). Notice that $\Sigma^{(i)}(\vec{p},\omega)$ have explicit nontrivial dependences on $\vec{p}$ and ω. This momentum dependence makes the calculation of the self-energy especially challenging in the presence of the dispersion anisotropy $v_F\neq v_\Delta$.

The critical theory depends on N and on the dispersion anisotropy $\alpha\equiv(v_F-v_\Delta)/v_F$. In the isotropic limit of $\alpha=0$, we obtained an analytic expression for the self-energy Eq. (4.4):[24]

$$\hat{\Sigma}(\vec{p},\omega) = \frac{(\omega\mathbb{I}-vp_x\tau_3+vp_y\tau_1)}{3\pi^2 N/4}\left[\frac{2}{3}+\ln\left(\frac{\Lambda^2}{-\omega^2+v^2|\vec{p}|^2}\right)\right] \tag{4.5}$$

for $v_F=v_\Delta=v$. Note, however, that this self-energy renormalizes v_Δ downward without affecting v_F. Since there is a loga-

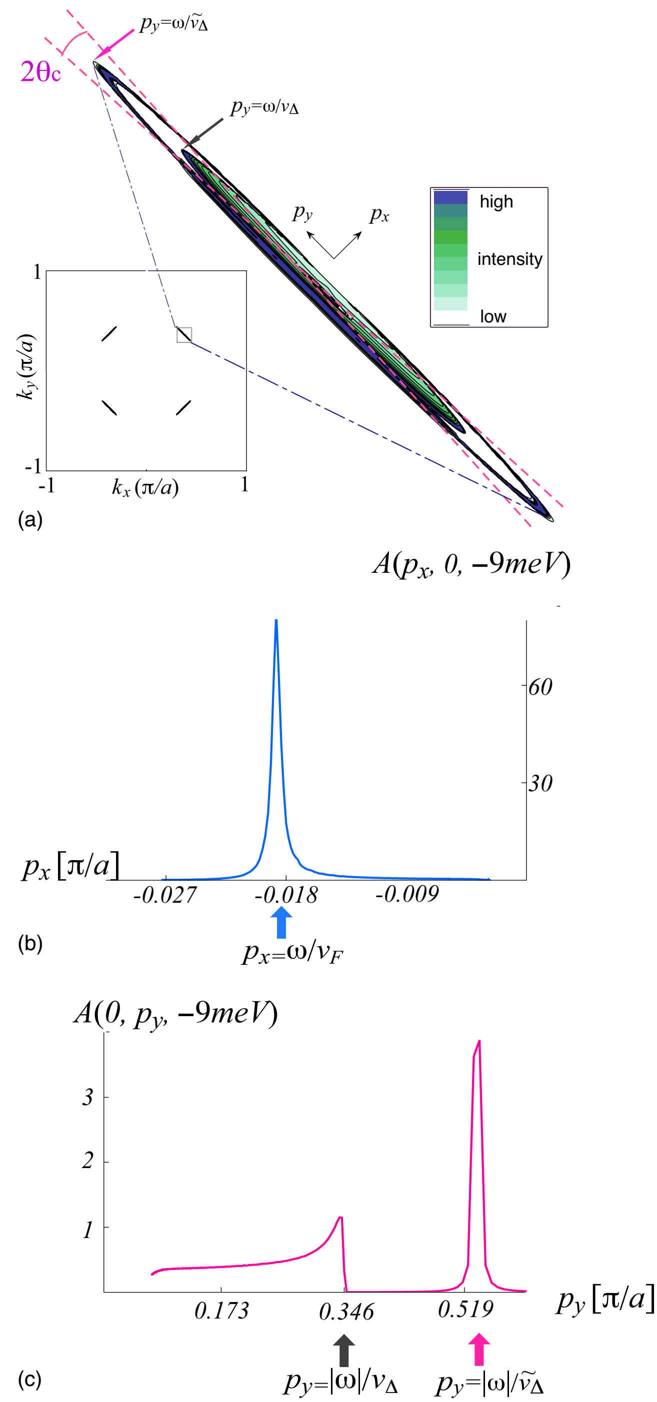

FIG. 3. (Color online) Momentum distribution of the nodal nematic QCP spectral function at an energy $\omega=-9$ meV for $v_F=0.508$ eV $(\pi/a)^{-1}$, $v_\Delta=0.026$ eV $(\pi/a)^{-1}$; $v_F/v_\Delta=19.5$. Here, the momentum $\vec{p}$ is measured with respect to nodal point $\vec{K}_1=(K,K)$ in a (rotated) local coordinate system, so that p_x and p_y lie, respectively, along the nodal and tangential directions. (a) Contour plot. θ_c is the critical angle at which a well defined qp peak departs from the incoherent continuum. For $\theta<\theta_c$, the qp is well defined. (b) and (c) are line cuts along the nodal direction and tangential direction, respectively.

rithmic divergence in this renormalization of v_Δ, the anisotropy ratio α is relevant at $\alpha=0$. Hence, it is clear that one should consider the case of an anisotropic dispersion $\alpha\neq 0$ from the beginning.

It is noteworthy that for any amount of anisotropy $\alpha\neq 0$, the analytic structure of the nodal fermion self-energy $\hat{\Sigma}(\vec{p},\omega)$ becomes qualitatively different from that at $\alpha=0$ given in Eq. (4.5). This is due to the existence of two energy scales $E_1(\vec{p})\neq E_2(\vec{p})$ [see Eq. (3.9) for the definition of these energy scales] entering the nematic mode propagator Eq. (3.8) (see Fig. 2). Such change in the analytic structure is not perturbatively accessible in α from the $\alpha=0$ case. Hence, we have numerically computed $\hat{\Sigma}$ from Eq. (4.4) for an arbitrary nonzero value of α by obtaining Im $\hat{\Sigma}$ via a Monte Carlo integration, and from this obtained Re $\hat{\Sigma}$ by Kramers–Kronig. We verified this method against the analytic expression Eq. (4.5) in the isotropic limit.

We present the nodal nematic QCP fermion spectral function $A(\vec{p},\omega)$, which was obtained from the numerical calculation of $\hat{\Sigma}(\vec{p},\omega)$, in Figs. 3 and 4. Although we have carried out the calculation for arbitrary values of velocities, we used the dispersion $v_F=0.508$ eV $(\pi/a)^{-1}$ and $v_\Delta=0.026$ eV $(\pi/a)^{-1}$ with the velocity ratio $v_F/v_\Delta=19.5$ in our plots in order to demonstrate the effect of a large bare velocity anisotropy. This dispersion was obtained by linearizing the phenomenological model Hamiltonian for BSCCO of Norman *et al.*[30] in our plots. For the value of the critical coupling, we used $\lambda_c^2/2N\gamma=0.3$. Figure 3 shows the momentum distribution of the spectral function at a fixed energy $\omega=-9$ meV. The eccentricity of the ellipses in the contour plot reflects the large bare velocity anisotropy. We also show two line cuts or momentum distribution curves (MDCs): one along the nodal direction and the other along the tangential direction. In Fig. 4, we show representative energy distribution curves (EDCs) at two fixed points in momentum space (one point along the nodal direction and another point along the tangential direction).

On the basis of this numerical calculation of $\hat{\Sigma}(\vec{p},\omega)$, and hence the spectral function $A(\vec{p},\omega)$, we extract two principal qualitative effects of the nematic critical fluctuations on the nodal Fermion properties: (i) strongly momentum (angle) dependent scattering and (ii) an anisotropic renormalization of the already anisotropic bare velocities.

The presence of strongly angle-dependent scattering is clearly shown in Fig. 3(a). The qps are highly damped in the direction normal to the FS (p_x direction) while they remain sharply defined in the vicinity of the FS (p_y direction). More specifically, the momentum distribution of the spectral intensity exhibits distinct behaviors in different wedges of p space, which open about the FS at a critical angle, $\theta_c=\tan^{-1}(v_\Delta/v_F)$. For $\theta>\theta_c$, the peaks in the spectral function are broad with a width $\propto|\omega|$. For $\theta<\theta_c$, the MDC has sharp peaks (the thin white lines) dispersing with a renormalized velocity $\tilde{v}_\Delta$, enhancing the eccentricity of the constant energy ellipse. We have marked the boundary between different wedges with dashed (pink) lines in Fig. 3(a). Due to the extreme bare anisotropy, the angle $2\theta_c$, which defines the region in $\vec{p}$ space with well defined qps, is rather small.

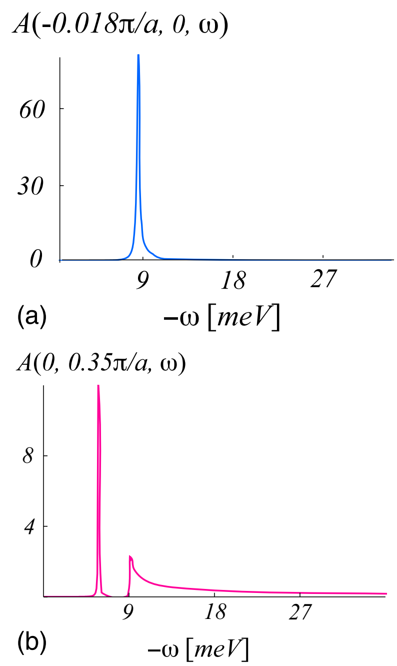

FIG. 4. (Color online) EDCs taken at two points in momentum space. (a) At $\vec{p}=(-9\text{ meV}/v_F,0)$. (b) At $\vec{p}=(0,9\text{ meV}/v_\Delta)$. These are the momenta corresponding to the position of the peak in Fig. 3(b) and to the threshold in Fig. 3(c), respectively.

However, this narrow wedge can qualitatively affect the long time properties of the nodal fermions.[35]

The anisotropic renormalization of the dispersion is particularly evident in Figs. 3(b) and 3(c). The free nodal fermion theory would have placed sharply defined peaks at $\vec{p}=(|w|/v_F,0)$ and $\vec{p}=(0,|w|/v_\Delta)$ in Fig. 3(b) and 3(c), respectively. Figure 3(b) indeed shows a peak (albeit broad) at the position expected from the bare value of the v_F, and hence, v_F is unrenormalized by $1/N$ fluctuations. However, the position of a sharp peak in Fig. 3(c) has been shifted away from the bare position. This shift is characterized by a renormalization of $v_\Delta\to\tilde{v}_\Delta$, where $\tilde{v}_\Delta$ is related to v_Δ by

$$\tilde{v}_\Delta=v_\Delta\left[1-\frac{1}{N}\Gamma\left(\frac{v_F}{v_\Delta}\right)-O\left(\frac{1}{N^2}\right)\right]. \qquad (4.6)$$

Here, $\Gamma(v_F/v_\Delta)$ is a positive function of v_F/v_Δ. As a result, critical fluctuations effectively enhance the dispersion anisotropy. Such anisotropic renormalization of the dispersion is the result of the structure of the coupling between the nematic mode and the nodal fermions and it holds order by order in the $1/N$ expansion.

One can readily understand the kinematic origins of the sharply defined qps near the FS inside the narrow wedge in Fig. 3(a). $E_1(\vec{p})$ defines the bare dispersion of a qp near the nodal point $\vec{K}_1=(K,K)$, while $E_2(\vec{p})$ defines the bare dispersion of a qp near the nodal point $\vec{K}_2=(K,-K)$. Since the coupling to qps near *both nodes* determines the dynamics of the nematic mode, it is the lesser of $E_1(\vec{p})$ and $E_2(\vec{p})$ that sets the threshold for decay. For $\vec{p}=(p_x,0)=(-9\text{ meV}/v_F,0)$ normal to the FS [Fig. 4(a)], $E_2(\vec{p})=v_\Delta|p_x|\ll E_1(\vec{p})=v_F|p_x|$, so the qp is highly damped. Notice the asymmetric line shape which reflects the $\vec{p}$ dependence of the self-energy. For $\vec{p}=(0,p_y)=(0,9\text{ meV}/v_\Delta)$ along the FS [Fig. 4(b)], the nematic fluctuations renormalize the qp velocity, $v_\Delta \to \tilde{v}_\Delta$, and the qp energy, $\tilde{E}_1(\vec{p})=\tilde{v}_\Delta|p_y|<E_1(\vec{p})\ll E_2(\vec{p})$, so there is no damping. It also produces an EDC with a "peak-dip-hump." The existence of *entirely* undamped quasiparticles inside sharply defined k-space wedges is likely an artifact of the first order corrections in the $1/N$ expansion since higher order terms are likely to introduce finite damping. It is therefore more plausible that the wedge delineates a crossover from a regime in which the qps are highly damped to a regime inside the wedge in which the qp peaks are relatively narrow with a width that vanishes as one approaches the tangential direction along the FS.

V. NEMATIC GLASS

Consider now the nodal nematic phase away from criticality, $\lambda > \lambda_c$, where the nematic order parameter has a nonzero expectation value, as in Eq. (3.5). Because of the Ising character of the ordered state, there is a gap in the nodal nematic fluctuation spectrum, $\omega_N \sim T_N \sim (\lambda_c - \lambda)$. At energies large compared to ω_N, the behavior of the spectral function differs little from its behavior at criticality. However, at energies small compared to ω_N, the nodal qps are undamped, but the nodal positions are shifted from the symmetric points in k space by an amount $\Delta p \propto \sqrt{\lambda - \lambda_c}$, as shown in Fig. 1 and the velocity tangential to the Fermi surface is renormalized, as in Eq. (4.6).

Unfortunately, quenched disorder (impurities) has a devastating effect on nematic phases, and indeed, macroscopic manifestations of electron nematic order have only been seen in ultrapure systems.[15,16] Specifically, the order parameter theory in the presence of impurities is equivalent to the random-field Ising model,[36,37] and hence, nematic systems are more generally expected to exhibit glassy dynamics rather than a broken symmetry.[38] Thus, more detailed spectroscopies and/or local measurements play an especially central role in experimental studies of nematic phases. Here, we sketch the effects of disorder on the single-particle spectral function in the nematic phases. We consider two extremal cases: short range and mesoscopic range disorder.

Short range disorder produces an imaginary part to the self-energy, which smears the MDC at $\omega=0$ in *all directions* about the nodal point. Due to the intrinsic dispersion anisotropy, this broadened weight is severely elongated along the tangential direction so the resulting MDC has a shape that resembles a Fermi "arc." However, the width of the MDC in the normal direction is still proportional to the arc length.

In sufficiently clean systems, the effects of disorder are only significant on longer distances, producing a "nematic glass." Here, we focus on the static effects, leaving out (important) dynamical effects generally expected in glassy phases, such as hysteresis and noise. If each domain is large enough to support a defined local nematic order, the variance $\sigma^2 \equiv \overline{|\langle\phi\rangle|^2}$ among domains amounts to a distribution of nodal positions along the FS. In such a mesoscale glass phase, a local measurement (such as STM) will see sharply defined nodal quasiparticles at low enough energy, but a measurement, such as ARPES, which averages over a large area, will measure the domain averaged spectral function:

$$\bar{A}(\vec{p},\omega) = \int d\phi P(\phi) A_0(p_x, p_y + \phi/v_\Delta, \omega), \tag{5.1}$$

where $P(\phi)$ is the probability density that ϕ will shift the position of the node by $\Delta p_y = \phi/v_\Delta$ and $A_0(p_x,p_y,\omega)$ is the spectral function for free qps:

$$A_0(p_x,p_y,\omega) = \frac{\pi}{E_1(\vec{p})}\{\delta(\omega - E_1(\vec{p}))[E_1(\vec{p}) + v_F p_x] + \delta(\omega + E_1(\vec{p}))[E_1(\vec{p}) - v_F p_x]\}, \tag{5.2}$$

with $E_1(\vec{p})$ given in Eq. (3.9). For a Gaussian distribution of ϕ with variance σ, $P(\phi)=e^{-\phi^2/2\sigma^2}/\sqrt{2\pi}\sigma$ and it is straightforward to show that the average spectral function in Eq. (5.1) becomes

$$\bar{A}(\vec{p},\omega) = \sqrt{\frac{\pi}{2\sigma^2}}\Theta[\omega^2 - (v_F p_x)^2]\frac{|\omega|}{\sqrt{\omega^2 - (v_F p_x)^2}} \times [e^{-(v_\Delta p_y - \sqrt{\omega^2 - (v_F p_x)^2})^2/2\sigma^2} + e^{-(v_\Delta p_y + \sqrt{\omega^2 - (v_F p_x)^2})^2/2\sigma^2}]. \tag{5.3}$$

Note that this defines a Fermi arc with length σ/v_Δ with a vanishing perpendicular width along the FS ($p_x=0$) at zero energy $\omega=0$.

VI. DISCUSSION

In this paper, we have presented a phenomenological theory of the nodal nematic QPT. Formally similar problems arise in studies of the nodal quasiparticles near other QPTs.[9,26,27] In all these cases, the ordered phase preserves the C_{4v} symmetry, and the velocity anisotropy is irrelevant so the fixed point is isotropic with emergent Lorenz invariance. In the case of a nodal nematic critical point, the dispersion anisotropy is enhanced at criticality. This has unforeseen effects on the single-particle spectral function.

We conclude with a few observations on the possible relevance of a nodal nematic quantum criticality to the cuprate physics, recognizing the danger of extrapolating large N results down to $N=2$. The previously cited evidence of a nematic phase $YBa_2Cu_3O_y$ near $y\sim 6.5$ from[1] transport anisotropy measurements and from inelastic neutron scattering in untwinned samples[3] involves studies of materials with unusual purity and crystalline perfection. Nematic order linearly couples to spatial inhomogeneity and disorder, which thus generically causes the ordered phase to be replaced by a glassy (domain) phase. A glassy phase with anisotropic domains has been seen in STM studies of underdoped $Bi_2Sr_2CaCu_2O_{8+\delta}$.[14] It is tempting to identify these structures and the "Fermi arcs" seen in ARPES experiments on the same material[39] with the nematic glass. However, this interpretation requires an extrapolation from the phase with strong SC order where the theory is valid to the nonsuperconducting pseudogap regime where the experiment is carried out. Moreover, this interpretation is far from unique.[40–42] A critical test of this interpretation is that as the disorder is made increasingly weak, there will be a crossover from a short range disorder behavior with a nodal point that is broadened in all direction to a nematic glass regime with a longer $T=0$ arc length but a narrower width [with Eq. (5.3) as the limiting case]. The existence of a nodal nematic phase,[43] which is related to ordered or fluctuating stripes, is moderately clear[6] in $La_{2-x}Sr_xCuO_4$ and related materials near $x=1/8$, but it seems likely that the critical phenomena in this system will considerably be affected by quenched disorder.

The structure of the single-particle spectral function at the nodal nematic QCP shown in Fig. 3 with sharp qps within a narrow wedge around the FS but otherwise broad may provide a consistent explanation for both the observation of broad qps in ARPES (Ref. 44) and of sharp qp interference peaks in STM (Refs. 45 and 46) on $Bi_2Sr_2CaCu_2O_{8+\delta}$. Since the wedge is so narrow due to the extreme dispersion anisotropy, it is unlikely to be observed in a direct momentum space probe. Hence, in ARPES, one is likely to only observe broad qps. However, the interpretation of peaks in the Fourier transform of STM on $Bi_2Sr_2CaCu_2O_{8+\delta}$ in terms of qp interference invoke the notion of coherent qps at the tips of the equal energy ellipses (or "bananas" as it is frequently referred to) along the FS.[45,46] The narrow wedge provides a natural and possibly unique mechanism for this interpretation. This aspect will be further analyzed in a future publication.[35]

ACKNOWLEDGMENTS

We thank E. Berg, A. Chubukov, H.-Y. Kee, M. Norman, A. Paramekanti, D. J. Scalapino, J. Tranquada, O. Vafek, M. Vojta, and E. Zhao for discussions. This work was supported in part by the NSF under Grants No. DMR 0442537 (E.F.) and No. DMR 0531196 (S.A.K.), by the DOE under Contracts No. DE-FG02-91ER45439 (E.F.) and No. DE-FG02-06ER46287 (S.A.K), by the Stanford Institute for Theoretical Physics (E.-A.K), and by the CRC (M.J.L.).

1. Y. Ando, K. Segawa, S. Komiya, and A. N. Lavrov, Phys. Rev. Lett. **88**, 137005 (2002).
2. V. Hinkov, D. Haug, B. Fauque, P. Bourges, Y. Sidis, A. Ivanov, C. Bernhard, C. T. Lin, and B. Keimer, Science **319**, 597 (2008).
3. V. Hinkov, P. Bourges, S. Pailhès, Y. Sidis, A. Ivanov, C. T. Lin, D. P. Chen, and B. Keimer, Nat. Phys. **3**, 780 (2007).
4. V. Hinkov, S. Pailhès, P. Bourges, Y. Sidis, A. Ivanov, A. Kulakov, C. T. Lin, D. P. Chen, C. Bernhard, and B. Keimer, Nature (London) **430**, 650 (2004).
5. H. A. Mook, P. C. Dal, F. Dogan, and R. D. Hunt, Nature (London) **404**, 729 (2000).
6. C. Stock, W. J. L. Buyers, R. Liang, D. Peets, Z. Tun, D. Bonn, W. N. Hardy, and R. J. Birgeneau, Phys. Rev. B **69**, 014502 (2004).
7. S. A. Kivelson, E. Fradkin, and V. J. Emery, Nature (London) **393**, 550 (1998).
8. S. A. Kivelson, I. P. Bindloss, E. Fradkin, V. Oganesyan, J. Tranquada, A. Kapitulnik, and C. Howald, Rev. Mod. Phys. **75**, 1201 (2003).
9. M. Vojta, Y. Zhang, and S. Sachdev, Phys. Rev. Lett. **85**, 4940 (2000).
10. M. Vojta, Y. Zhang, and S. Sachdev, Int. J. Mod. Phys. B **14**, 3719 (2000).
11. S. Sachdev, Rev. Mod. Phys. **75**, 913 (2003).
12. M. Matsuda, M. Fujita, S. Wakimoto, J. A. Fernandez-Baca, J. M. Tranquada, and K. Yamada, arXiv:0801.2254 (unpublished).
13. C. Howald, H. Eisaki, N. Kaneko, and A. Kapitulnik, Proc. Natl. Acad. Sci. U.S.A. **100**, 9705 (2003).
14. Y. Kohsaka, C. Taylor, K. Fujita, A. Schmidt, C. Lupien, T. Hanaguri, M. Azuma, M. Takano, H. Eisaki, H. Takagi, S. Uchida, and J. C. Davis, Science **315**, 1380 (2007).
15. K. B. Cooper, M. P. Lilly, J. P. Eisenstein, L. N. Pfeiffer, and K. W. West, Phys. Rev. B **65**, 241313(R) (2002).
16. R. A. Borzi, S. A. Grigera, J. Farrell, R. S. Perry, S. J. S. Lister, S. L. Lee, D. A. Tennant, Y. Maeno, and A. P. Mackenzie, Science **315**, 214 (2007).
17. In an upcoming paper of Y. Huh and S. Sachdev, the nature of the fixed point to order $1/N$ is studied, and it is found that there are logarithmically slow flows to infinite anisotropy. Moreover, it is found that large anisotropy serves the same role in the theory as large N, thus giving corroborating evidence that the large N results may be applied to the physical case of $N=2$.
18. A similar approach was taken for a study of $d \to d + id$ QPT by D. V. Khveshchenko and J. Paaske, Phys. Rev. Lett. **86**, 4672 (2001).
19. K. G. Wilson, Phys. Rev. D **7**, 2911 (1973).
20. D. J. Gross and A. Neveu, Phys. Rev. D **10**, 3235 (1974).
21. J. Zinn-Justin, *Quantum Field Theory and Critical Phenomena* (Oxford University Press, Oxford, 1993).
22. M. Moshe and J. Zinn-Justin, Phys. Rep. **385**, 69 (2003).
23. John L. Cardy, *Scaling and Renormalization in Statistical Physics* (Cambridge University Press, Cambridge, 1996).
24. E.-A. Kim *et al.* (unpublished).
25. L. Balents, M. P. A. Fisher, and C. Nayak, Int. J. Mod. Phys. B **12**, 1033 (1998).
26. O. Vafek, Z. Tešanović, and M. Franz, Phys. Rev. Lett. **89**, 157003 (2002).
27. M. Hermele, T. Senthil, and M. P. A. Fisher, Phys. Rev. B **72**, 104404 (2005).
28. These two results are not necessarily in contradiction with each other. What they mean is that the quantum phase transition is first order for small ϵ and finite N, while it is continuous at large N and fixed dimension. In the ϵ-N plane, the first order and continuous phase transition regions should then coalesce as $\epsilon \to 0$ and $N \to \infty$, and the order of limits does not commute.
29. M. Chiao, R. W. Hill, C. Lupien, L. Taillefer, P. Lambert, R. Gagnon, and P. Fournier, Phys. Rev. B **62**, 3554 (2000).
30. M. R. Norman, M. Randeria, H. Ding, and J. C. Campuzano, Phys. Rev. B **52**, 615 (1995).
31. E. Fradkin, *Field Theories of Condensed Matter Systems* (Addison-Wesley, Redwood, 1991).

[32] Nonquadratic correlators of the nematic fluctuations φ are infrared singular at the QPT (Ref. 24). This is common for Dirac fermions (Refs. 19, 21, and 22) and in ferromagnetic metals (Ref. 33). The main effect of these infrared singular corrections is to change, order by order in $1/N$, the critical exponents of this system.

[33] J. Rech, C. Pépin, and A. V. Chubukov, Phys. Rev. B **74**, 195126 (2006).

[34] Analogous scaling occurs in other theories of relativistic fermions coupled to scalar fields (Refs. 21 and 22).

[35] E.-A. Kim and M. J. Lawler (unpublished).

[36] E. W. Carlson, K. A. Dahmen, E. Fradkin, and S. A. Kivelson, Phys. Rev. Lett. **96**, 097003 (2006).

[37] T. Nattermann, in *Spin Glasses and Random Fields*, edited by A. Young (World Scientific, Singapore, 1998).

[38] J. P. Sethna, K. A. Dahmen, and O. Perković, in *Science of Hysteresis*, edited by I. D. Mayergoyz and G. Bertotti (Academic, London, 2004).

[39] A. Kanigel, M. Norman, M. Randeria, U. Chaterjee, S. Souma, A. Kaminski, H. M. Fretwell, S. Rosenkranz, M. Shi, T. Sato, T. Takahashi, Z. Li, H. Raffy, K. Kadowaki, D. Hinks, L. Ozyuzer, and J. C. Campuzano, Nat. Phys. **2**, 447 (2006).

[40] C. M. Varma and L. Zhu, Phys. Rev. Lett. **98**, 177004 (2007).

[41] A. Paramekanti and E. Zhao, Phys. Rev. B **75**, 140507(R) (2007).

[42] E. Berg and E. Altman, Phys. Rev. Lett. **99**, 247001 (2007).

[43] T. Valla, A. V. Fedorov, J. Lee, J. C. Davis, and G. D. Gu, Science **314**, 1914 (2006).

[44] A. Damascelli, Z. Hussain, and Z. X. Shen, Rev. Mod. Phys. **75**, 473 (2003).

[45] K. McElroy, R. W. Simmonds, J. E. Hoffman, D. H. Lee, J. Orenstein, H. Eisaki, S. Uchida and J. C. Davis, Nature (London) **422**, 592 (2003).

[46] Q.-H. Wang and D.-H. Lee, Phys. Rev. B **67**, 020511(R) (2003).